analytical chemistry

Article

pubs.acs.org/ac

Open Access on 05/16/2015

High Temporal Resolution Measurements of Dopamine with Carbon Nanotube Yarn Microelectrodes

Christopher B. Jacobs,[†] Ilia N. Ivanov,[‡] Michael D. Nguyen,[†] Alexander G. Zestos,[†] and B. Jill Venton*[,†]

[†]Department of Chemistry, University of Virginia, McCormick Road, Box 400319, Charlottesville, Virginia 22904-4319, United States

[‡]Center for Nanophase Materials Sciences, Oak Ridge National Laboratory, 1 Bethel Valley Road Bld. 8610, Rm. M166, Oak Ridge, Tennessee 37831, United States

Supporting Information

ABSTRACT: Fast-scan cyclic voltammetry (FSCV) can detect small changes in dopamine concentration; however, measurements are typically limited to scan repetition frequencies of 10 Hz. Dopamine oxidation at carbon-fiber microelectrodes (CFMEs) is dependent on dopamine adsorption, and increasing the frequency of FSCV scan repetitions decreases the oxidation current, because the time for adsorption is decreased. Using a commercially available carbon nanotube yarn, we characterized carbon nanotube yarn microelectrodes (CNTYMEs) for high-speed measurements with FSCV. For dopamine, CNTYMEs have a significantly lower ΔE_p than CFMEs, a limit of detection of 10 ± 0.8 nM, and a linear response to 25 μM. Unlike CFMEs, the oxidation current of dopamine at CNTYMEs is independent of scan repetition frequency. At a scan rate of 2000 V/s, dopamine can be detected, without any loss in sensitivity, with scan frequencies up to 500 Hz, resulting in a temporal response that is four times faster than CFMEs. While the oxidation current is adsorption-controlled at both CFMEs and CNTYMEs, the adsorption and desorption kinetics differ. The desorption coefficient of dopamine-*o*-quinone (DOQ), the oxidation product of dopamine, is an order of magnitude larger than that of dopamine at CFMEs; thus, DOQ desorbs from the electrode and can diffuse away. At CNTYMEs, the rates of desorption for dopamine and dopamine-*o*-quinone are about equal, resulting in current that is independent of scan repetition frequency. Thus, there is no compromise with CNTYMEs: high sensitivity, high sampling frequency, and high temporal resolution can be achieved simultaneously. Therefore, CNTYMEs are attractive for high-speed applications.

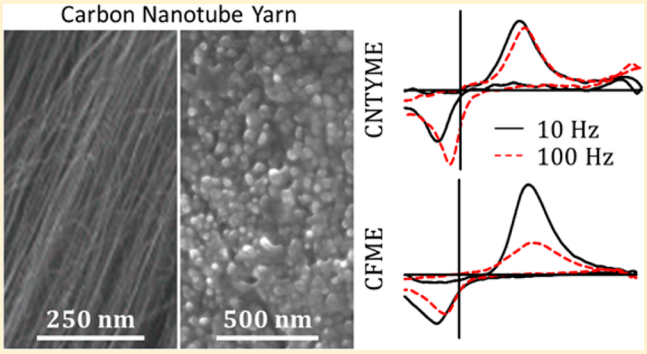

Carbon fibers (CFs) are one of the most common microelectrode materials for electrochemical detection of neurotransmitters because of their small diameter, electrochemical properties, adsorption affinity for cationic neurotransmitters, and compatibility with fast electrochemical methods.[1−6] Carbon-fiber microelectrodes (CFMEs), coupled with constant potential amperometry, can perform sensitive, high temporal resolution measurements;[7−10] however, the intrinsic lack of analyte selectivity limits the usefulness of amperometry to instances in which the analyte identity is already known. Thus, amperometry has limited utility in chemically complex environments. Measurements in environments such as the intact brain, where a mixture of chemicals could be present, require a technique that provides chemical identification. Fast-scan cyclic voltammetry (FSCV) has become a preferred method for *in vivo* measurements, because it provides a chemical fingerprint that aids in chemical identification.[6,11−15] The sensitivity for cationic neurotransmitters, such as dopamine, using FSCV is typically limited by adsorption onto the electrode surface, and increasing the scan repetition frequency dramatically decreases the electrode sensitivity. This necessitates a compromise between the sampling frequency of the measurements and the sensitivity. Typically, a scan repetition frequency of 10 Hz is used as the optimal sampling frequency.[16−18] However, a recent study compared FSCV scan frequencies at 10 and 60 Hz and found that measurements taken at 10 Hz significantly underestimate rapid uptake rates.[1] Thus, in order to characterize rapid concentration changes *in vivo*, the sampling frequency and the temporal resolution of neurotransmitter detection must be improved.

Carbon nanotubes (CNTs) are a promising microelectrode material, because of the rapid electron transfer kinetics and the increased sensitivity demonstrated at larger CNT-based electrodes.[19−21] Electrodes incorporating CNTs have been made by modifying the CFME surface with CNTs through a dip-coating process,[22,23] using a polymer-CNT matrix fiber as the electroactive material,[24] and by the synthesis of aligned

Received: December 14, 2013
Accepted: May 16, 2014
Published: May 16, 2014

   dx.doi.org/10.1021/ac404050t | *Anal. Chem.* 2014, 86, 5721−5727

CNT arrays on larger silicon or metal substrates.[19,25−27] Dip-coating procedures apply a film of randomly oriented CNTs on the electrode surface, but these films are often heterogeneous in thickness and a large portion of the exposed CNT surface is sidewall. The oxide functional groups primarily responsible for the adsorption of neurotransmitters are more prevalent at defect sites and at CNT ends than on CNT sidewalls. To maximize neurotransmitter adsorption sites, arrays of vertically aligned CNTs are preferred, but the resulting electrodes are often on the millimeter scale, which is too large for implantation into tissue.[17,20,28,29] As an alternative, CNTs have been aligned on an electrode surface with chemical self-assembly, resulting in an electrode with significantly higher sensitivity toward dopamine.[30] Similar to CFMEs, the sensitivity of these carbon nanotube forest electrodes decreases as the repetition frequencies increase; however, the electrodes have a greater sensitivity, so a 90 Hz scan frequency could detect signals similar to bare CFMEs at 10 Hz.[30] While CNT-based microelectrodes have some promising characteristics the fabrication of reliable and reproducible microelectrodes has been challenging. Thus, CNT-based materials have not been routinely used as a replacement for CFs.

In this paper, we explore the use of carbon nanotube yarns (CNTYs) as an electrode material for enhanced neurotransmitter detection. CNTYs typically range from 10 μm to 50 μm in diameter and are commercially available for industrial purposes in lengths up to several kilometers long.[31−34] Various types of CNTYs have been used for deep brain stimulation,[35] in glucose enzyme sensors,[36−39] and for detection of dopamine in brain slices.[40] Here, we investigate the use of CNTY microelectrodes (CNTYMEs) for high-frequency measurements of dopamine, resulting in increased temporal resolution. The adsorption and desorption of dopamine (DA) and dopamine-*o*-quinone (DOQ) at CNTYMEs differ dramatically from those at traditional CFMEs, which facilitates FSCV measurements of dopamine at 500 Hz without a loss in sensitivity. The ability to make high-frequency measurements at CNTYMEs is a substantial benefit over CFMEs and makes CNTYMEs attractive for high-speed applications.

EXPERIMENTAL SECTION

Solutions. Dopamine hydrochloride and potassium hexachloroiridate(IV) (K_2IrCl_6) were purchased from Sigma−Aldrich (St. Louis, MO). Ten millimolar (10 mM) stock solutions of the analytes were prepared in $HClO_4$, and were diluted daily to the desired concentration in Tris-buffer (15 mM tris(hydroxymethyl)aminomethane, 3.25 mM KCl, 140 mM NaCl, 1.2 mM $CaCl_2$, 1.25 mM NaH_2PO_4, 1.2 mM $MgCl_2$, and 2.0 mM Na_2SO_4, with the pH adjusted to 7.4).

Carbon Nanotube Yarn Microelectrode Preparation. A length of commercially available CNTY 10−25 μm in diameter, 1−2 cm long, (General Nano, LLC, Cincinnati, OH) was either (1) inserted into a polyimide coated fused-silica capillary while submerged in 2-propanol, to reduce friction and ease insertion (45 μm inner diameter (ID) × 90 μm outer diameter (OD), Polymicro Technologies, Phoenix, AZ),[41] or (2) inserted into a 0.68 mm ID × 1.2 mm OD glass capillary that had previously been pulled into a glass pipet and cut to have an opening diameter of ∼50 μm. The solvent was allowed to fully evaporate from inside of the capillary before the CNTY was sealed into the capillary with Loctite brand 5 min epoxy and was allowed to fully cure for 24 h. The resulting microelectrode was polished at an ∼90° angle on a Sutter Instruments polishing wheel with subsequent coarse and fine polishing disks to make a disk CNTYME. For comparison, carbon fiber microelectrodes (CFMEs) were also fabricated, insulated, and polished in a similar manner using 7-μm-diameter T-650 carbon fibers (Cytec Technologies, Woodland Park, NJ).[22]

Electrochemistry. FSCV was performed with a custom built instrument and a ChemClamp potentiometer (Dagan, Minneapolis, MN, n = 0.01 headstage), PCI 6711 and 6052 computer interface cards (National Instruments, Austin, TX) and home-built breakout box. Electrodes were backfilled with 1 M KCl and a silver wire was inserted to connect the electrode to the potentiostat headstage. The typical triangular waveform swept the applied potential from −0.4 V to 1.3 V at 400 V/s versus a Ag/AgCl reference electrode, at a scan frequency of 10 Hz, except where noted. Data collection was computer-controlled by the TarHeel CV software program.[12]

Electrodes were tested using a flow-injection system, as previously described.[42] Analyte injections lasting 4 s were made and the current versus time traces were obtained by integrating the current in a 100 mV window centered at the oxidation peak for each cyclic voltammogram (CV). Background-subtracted CVs were calculated by subtracting the average of 10 background scans, taken before the compound was injected, from the average of five CVs recorded after the analyte bolus was injected.

Surface Characterization. Detailed information on the electron microscopy techniques and the Raman spectroscopy instrumentation can be found in the Supporting Information.

Statistics. GraphPad Prism 4.0 was used for all statistics (GraphPad Software, San Diego, CA). All averaged values are given as the mean ± SEM (standard error of the mean) for "n" number of electrodes, unless otherwise noted. Normalized signals were calculated for individual electrodes before being averaged. Significance is defined as p = 0.05.

RESULTS AND DISCUSSION

Surface Characterization. Carbon nanotube yarns (CNTYs) consist of two or more multiwalled CNT (MWCNT) threads twisted together, each typically ∼5 μm in diameter. Because multiple threads are twisted together, CNTYs do not have perfectly circular cross sections, and often have localized areas that vary in CNT density.[31,34] The cross-section of the CNTY typically ranges between 5 μm and 25 μm, but microelectrode fabrication in pulled glass capillaries can yield carbon nanotube yarn microelectrodes (CNTYMEs) with electrode tips smaller than the original measured cross-section of the CNTY, because the yarn can compress.[43] The SEM image in Figure 1A shows an example of a pulled glass capillary disk microelectrode, with a tip diameter of 10 μm. High-magnification SEM images of the CNTYME surface (Figure 1B) shows a multitude of small circles, each about 30 nm in diameter, which suggests that the surface consists primarily of CNT ends.

To further characterize the CNT surface, Raman spectra of freshly prepared electrodes were measured. A characteristic Raman spectrum of the CNTYME shows first- and second-order peaks between 1000 cm^{-1} and 2800 cm^{-1} (Figure 1C). The double resonance feature of the D-band peak (1328 cm^{-1}) gives information on the density of the defects in the CNTs, as well as the MWCNT diameter if MWCNT are aligned.[44,45] The second prominent first-order feature is the G-band (1582 cm^{-1}), which is common for all graphitic carbon structures.

dx.doi.org/10.1021/ac404050t | Anal. Chem. 2014, 86, 5721−5727

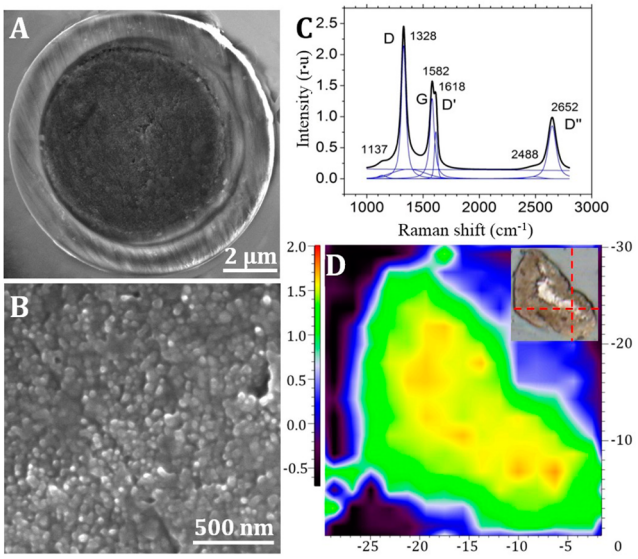

Figure 1. Surface characterization of a carbon nanotube yarn microelectrode (CNTYME): (A) SEM image of the polished surface of a CNTYME fabricated in a pulled-glass capillary; (B) SEM image of the electrode surface shows the ends of individual 30−50 nm diameter CNTs bundled tightly together to form a nanostructured surface; (C) Raman spectrum shows first-order features of a peak at 1328 cm^{-1} (D-band, generally associated with defects), at 1582 cm^{-1} (G-band, the high-frequency E_{2g} first-order mode), and a peak at 1618 cm^{-1} (D′-band, which can be explained by double-resonance theory. (Two double resonance features observed as a shoulder at 2488 cm^{-1} and a prominent band at 2652 (D″ band).) (D) The relative ratio of D to G band intensities. (A false color map of the calculated D/G-band intensity ratio across the CNTY electrode surface shows a surface with many defects, particularly in the central part of the electrode.) The optical image of the CNTYME surface (inset) reveals the typical noncircular shape of the CNT yarn that corresponds to the spectroscopic Raman surface map. Red lines indicate the point where the spectrum in panel (C) was taken.

The high intensity peak at 1618 cm^{-1} could be due to the D′-band of carbon nanotubes; however, the D′ peak of MWCNTs is usually weak with the 632 nm detection used here and only becomes prominent under NIR excitation of 1064 nm.[45] The 1618 cm^{-1} peak may also be attributed to the delamination of graphitic carbon caused by adjacent oxide functional groups.[46−49] A double resonance feature of the D″ peak (2650 cm^{-1}) and a shoulder band at 2488 cm^{-1} were also observed.

The D and G band features were further analyzed because the nature of these bands is better understood. The full width at half-maximum (fwhm) of the D band is 48 cm^{-1} and can be used to estimate the CNT diameter by calibration of the D-band fwhm, as a function of $1/d$.[44] Assuming the microelectrode surface primarily consists of CNT ends aligned perpendicular to the laser polarization, the diameter is estimated to be 29 nm. If the CNT ends were pulled out from the yarn enough to bend and become parallel to the laser polarization, then the diameter would be 57 nm instead. Transmission electron microscopy (TEM) (see Figure S-2 in the Supporting Information), verified the CNT diameters range from ∼20 nm to 40 nm, with the majority being ∼30 nm. The agreement in diameter between the TEM measurement and the Raman data suggest that the electrode surface consists primarily of CNT ends and not CNT sidewalls. The Raman map of absolute G-band intensity (Figure S-2 in the Supporting Information) suggests that the CNT density is higher at the center of the yarn, which is consistent with previous studies on CNTY structure.[31,34] A false-color map of the ratio of I_D/I_G-band intensity (Figure 1D) reveals variation in defect density across the surface.[50,51] The entire CNTYME surface has a I_D/I_G band ratio higher than 1, which indicates that the entire surface is defect-rich. Pristine CNT samples would be expected to yield very low I_D/I_G-band ratios of $\ll$1.

Electrochemical Characterization. Figure 2 compares dopamine redox at a CNTYME (Figure 2A) and a CFME

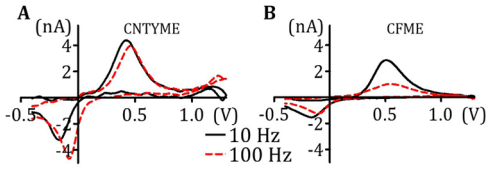

Figure 2. Comparison of the effect of FSCV scan repetition rate at (A) a carbon nanotube yarn disk microelectrode (CNTYME) and (B) a carbon fiber disk microelectrode (CFME). One micromolar (1 μM) dopamine is detected using a scan rate of 400 V/s. The repetition rate is either 10 Hz (solid black traces) or 100 Hz (dashed red traces).

(Figure 2B) using the typical FSCV waveform scanning from −0.4 V to 1.3 V and back at 400 V/s and a scan repetition frequency of 10 Hz (solid black lines). The general shape of the CVs are similar, but the CNTYME displays a sharper oxidation peak ($i_{p,a}$) and reduction peak ($i_{p,c}$) than the CFME. The potential difference between the oxidation and reduction peak voltages (ΔE_p) is smaller at the CNTYME, implying that it may have faster electron transfer kinetics than the CFME.

The measured current for dopamine oxidation is linear up to 25 μM and the limit of detection for dopamine was determined to be 8 ± 1 nM (n = 8) at CNTYMEs, indicating that CNTYMEs are suitable for detecting low concentrations of dopamine (see Figure S-4 in the Supporting Information). The Sombers laboratory utilized a different CNT yarn for dopamine detection and found an LOD of 13 ± 2 nM, which is similar to our measurements.[40] This suggests that our microelectrodes using the commercially available CNT yarns have sensitivities that are similar to the previously investigated CNTY microelectrodes, even though the CNT yarn materials are not identical. However, the effect of increased scan repetition frequency at CNTYMEs was not been investigated.

Increasing the repetition rate from 10 Hz to 100 Hz reduces the time between scans from 91.5 ms to 1.5 ms, respectively, dramatically reducing the time for dopamine to adsorb to the electrode surface. The red, dashed traces in Figure 2 show CVs measured with a scan repetition frequency of 100 Hz at the same electrode as the 10 Hz traces. The oxidation and reduction currents at the CFME decreases with the 100 Hz repetition rate (Figure 2B). At the CNTYME (Figure 2A), however, CVs at both frequencies have almost-identical oxidation currents.

Figures 3A and 3B show the effect of repetition frequency on the average peak oxidation current (normalized to the peak current at 10 Hz for each electrode). At CFMEs, $i_{p,a}$ decreases dramatically as the repetition rate is increased; doubling the repetition rate from 10 Hz to 20 Hz reduces the current by 40% and increasing the repetition frequency to 110 Hz decreases the $i_{p,a}$ by 78%. At CFMEs, this trend had a slope of −0.59 ± 0.05 and was significantly nonzero (p < 0.0001, n = 4). In contrast,

dx.doi.org/10.1021/ac404050t | Anal. Chem. 2014, 86, 5721−5727

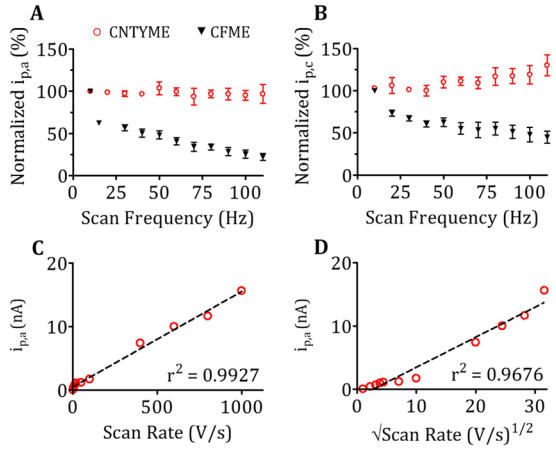

Figure 3. Effect of scan repetition frequency on dopamine measurement at CNTYME and CFMEs: (A) peak oxidation current, and (B) peak reduction current at CNTYMEs (red circles, n = 10) and CFMEs (black triangles, n = 4). Peak currents were normalized to the current at 10 Hz, and error bars represent the standard error of the mean. (C) Oxidation current for a CNTYME for 1 μM dopamine plotted against (C) scan rate and (D) the square root of scan rate. The linearity between dopamine oxidation current and scan rate indicates that dopamine oxidation is surface-dependent at CNTYMEs.

the oxidation current at CNTYMEs does not change between 10 Hz and 110 Hz, and the slope of the trend line is 0.03 ± 0.05 for CNTYME, which was not significantly different from zero (p = 0.5323, n = 10). Although the surface is heterogeneous, the trend of scan-frequency-independent current was consistent across electrodes. Seventy percent (70%) of CNTYMEs had no change in current with frequency and ∼30% displayed either a slight increase or decrease in current; however, the oxidation current did not change by more than 20% at any CNTYME. Thus, the oxidation current is dependent on scan frequency at CFMEs but is frequency independent at CNTYMEs. The reduction currents have similar trends as the oxidation currents (Figure 3B); they do not decrease at higher scan frequencies at CNTYMEs, but they do at CFMEs.

Previous studies of CNT microelectrodes did not observe a current that was independent of scan frequency.[30] At CNT forest electrodes, where CNTs were attached to CFMEs using chemical self-assembly, the oxidation current decreases with increasing frequency, similar to CFMEs.[30] The alignment of CNTs in the yarns may be better than in the chemical self-assembly method, leading to more CNT ends exposed and a different surface for adsorption.

The temporal response of dopamine oxidation at CFMEs and CNTYMEs is compared by measuring the time required for the signal to change from 10% to 90% of the maximum oxidation current after the injection of a dopamine bolus. The time response is dependent on the electrode material and the scan repetition frequency. CFMEs, at the typical scan rate of 400 V/s, yield a time response of 1.2 ± 0.2 s with a 10 Hz scan frequency, which decreases to 0.6 ± 0.2 s at a scan frequency of 110 Hz. Since the current decreases by over 75% at a scan frequency of 110 Hz, the improved temporal resolution at high scan frequencies comes with a great tradeoff in sensitivity. Using the 400 V/s scan rate at CNTYMEs, the temporal response of dopamine detection is 0.45 ± 0.09 s at 10 Hz and is further improved to 0.27 ± 0.09 s at 110 Hz. The scan frequency does not affect the current at CNTYMEs, thus the faster time response at higher frequencies can be utilized without compromising sensitivity. Both the sampling frequency and the temporal response for dopamine detection can be improved by almost an order of magnitude utilizing CNTYMEs instead of CFMEs.

Adsorption Mechanism and Kinetic Modeling. Scan rate was varied to determine whether dopamine kinetics at CNTYMEs are limited by diffusion or adsorption. For a diffusion-limited process, $i_{p,a}$ is linear with the square root of scan rate; however, for an adsorption-limited process, $i_{p,a}$ is linear with scan rate.[52] Figures 3C and 3D show that oxidation current is linear with scan rate and is not linear with the square root of scan rate at CNYMEs, indicating that it is a surface-dependent process. The outer-sphere oxidation of $IrCl_6^{3-}$ is linear with the square root of scan rate at CNYMEs (see Figure S-3 in the Supporting Information) denoting that this process is diffusion-limited, and confirming that the CNTYME behaves as expected to a surface-independent analyte.[53] Since both CNTYMEs and CFMEs are rate limited by adsorption, we hypothesized that there must be a difference in the adsorption/desorption properties between the two microelectrode materials.

The Wightman group developed a model of FSCV data to determine the rate constants for the adsorption and desorption kinetics of dopamine (DA) at CFMEs.[54] Briefly, the equilibrium reactions between the electrode surface and the DA or dopamine-o-quinone (DOQ) in solution are described by

$$DA_{Sol'n} \underset{k_{-1}}{\overset{k_1}{\rightleftharpoons}} DA_{Ads} \overset{-2e^-}{\rightleftharpoons} DOQ_{Ads} \underset{k_{-2}}{\overset{k_2}{\rightleftharpoons}} DOQ_{Sol'n}$$

where k_1 and k_2 are the adsorption rate constants of DA and DOQ, respectively, and k_{-1} and k_{-2} are the respective desorption rate constants. During the anodic scan, adsorbed

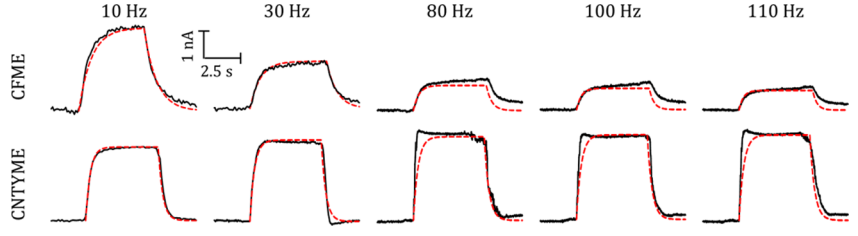

Figure 4. Measured current versus time traces of 1 μM dopamine bolus injection at a CNTYME and a CFME (solid, black traces) and the best-fit simulation (dotted, red traces) used to characterize the adsorption and desorption rate constants. The simulation parameters for this example CFME are $k_1 = 5.9 \times 10^{-3}$ cm s^{-1}, $k_2 = 6.6 \times 10^{-3}$ cm s^{-1}, $k_{-1} = 0.84$ s^{-1}, and $k_{-2} = 6.1$ s^{-1}; the simulation parameters for CNTYME are $k_1 = 10.1 \times 10^{-3}$ cm s^{-1}, $k_2 = 10.1 \times 10^{-3}$ cm s^{-1}, $k_{-1} = 4.15$ s^{-1}, and $k_{-2} = 4.03$ s^{-1}. FSCV scan parameters: from −0.4 V to 1.3 V and back at 400 V/s vs AglAgCl.

dx.doi.org/10.1021/ac404050t | Anal. Chem. 2014, 86, 5721−5727

Table 1. Average Rate Constants and Kinetic Values for 1 μM Dopamine

1 μM DA	n	k_1 (10^{-3} cm s^{-1})	k_2 (10^{-3} cm s^{-1})	k_{-1} (s^{-1})	k_{-2} (s^{-1})	ΔE_p (mV)	$i_{p,c}/i_{p,a}$
CFME	4	6 ± 1	6 ± 1	0.8 ± 0.03	15 ± 3	680 ± 5	0.63 ± 0.01
CNTYME	5	10 ± 3	10 ± 5	4.1 ± 0.05	4.0 ± 0.1	580 ± 3	0.77 ± 0.01

dopamine is oxidized to DOQ, which can remain adsorbed to the surface or desorb from the electrode. DOQ that remains on the electrode surface is reduced back to dopamine during the cathodic scan. If DOQ desorbs prior to the cathodic scan, the reduction current is smaller than the oxidation current.

During flow injection experiments, a bolus of analyte flows past the electrode. If the oxidation is surface independent, the current versus time trace would be square-shaped; i.e., the oxidation current would rise to the highest value at the introduction of dopamine and would return to baseline immediately at the end of the bolus. However, for an adsorption-limited species, such as dopamine, the concentration at the electrode surface requires time to reach equilibrium after the introduction of DA. Thus, the current versus time response is slowed and the curve is rounded, and both adsorption and desorption parameters can be extracted from the shape of the curve. Current versus time curves for 1 μM dopamine measured at five distinct scan frequencies, between 10 Hz and 110 Hz, were simultaneously modeled to determine the adsorption and desorption rate constants for CFMEs and CNTYMEs. Figure 4 compares the measured current vs time curves (solid, black) to the best-fit simulation curves (dashed, red). There is a good fit between the model and measured curves at all five frequencies ($r^2 > 0.9650$). The adsorption constants for DA and DOQ are similar to each other at both CFMEs ($k_1 \approx k_2 \approx 6 \times 10^{-3}$ cm/s) and CNTYMEs ($k_1 \approx k_2 \approx 10 \times 10^{-3}$ cm/s). The desorption values of DA and DOQ at CFMEs differ by almost an order of magnitude, with DOQ desorbing faster ($k_{-1} = 0.8$ s^{-1} vs $k_{-2} = 15$ s^{-1}). However, at CNTYMEs, the rate constants for the desorption of DA and DOQ were nearly identical ($k_{-1} = 4.2$ s^{-1} and $k_{-2} = 4.0$ s^{-1}).

The average rate constants for CFMEs and CNTYMEs are in Table 1. At each type of electrode, the adsorption constants for dopamine and DOQ are similar to each other, even though the specific values are different for CFMEs and CNTYMEs. At CNTYMEs, the rates of desorption for DA and DOQ are almost identical, while at CFMEs, the rate of desorption for DOQ is over an order of magnitude higher than that for DA. The desorption constants vary less between electrodes than the adsorption constants, implying that desorption may not be as surface-area-dependent as the adsorption.

The calculated equilibrium constant for dopamine at CFMEs is $K_1 = 7.0 \times 10^{-3} \pm 1 \times 10^{-3}$ cm and for DOQ is $K_2 = 0.4 \times 10^{-3} \pm 0.4 \times 10^{-3}$ cm, indicating that adsorption of dopamine occurs more readily than DOQ to the surface. At CNTYME, K_1 (dopamine) $= 2.6 \times 10^{-3} \pm 0.4 \times 10^{-3}$ cm and K_2 (DOQ) $= 3.0 \times 10^{-3} \pm 0.5 \times 10^{-3}$ cm, indicating that both compounds have similar equilibrium coefficients and thus similar adsorption affinities. The equilibrium coefficients at CNTYMEs fall between the K_1 and K_2 values at CFMEs, indicating that the adsorption of DA at CNTYMEs is not as strong as the adsorption of DA at CFMEs, and that the adsorption of DOQ is stronger at CNTYMEs compared to CFMEs. The similarity between K_1 and K_2 at CNTYMEs also suggests that dopamine oxidation is also more reversible at CNTYMEs than at CFMEs.

In order for DOQ to be reduced back to dopamine during the cathodic scan, DOQ must remain adsorbed to the surface. At CFMEs, the DOQ desorption rate constant is substantially higher than for dopamine, so the DOQ leaves the electrode surface more readily and the reduction peak is smaller than the oxidation peak. The average peak current ratio (Table 1) shows that the reduction current is only ~60% of the oxidation current at CFMEs. On average, $i_{p,c}/i_{p,a}$ is larger at CNTYMEs than CFMEs (0.77 ± 0.01 and 0.62 ± 0.01, respectively), indicating that dopamine oxidation is more reversible at CNTYMEs. This increase in reversibility also confirms the modeling data that the adsorption/desorption kinetics are different between the two electrode materials.

The overpotential values for both oxidation and reduction of dopamine are significantly reduced at CNTYMEs, yielding a peak separation (ΔE_p) that is ~90 mV lower than at CFMEs (scan rate = 400 V/s, Table 1, $p = 0.001$, paired t-test). The reduced ΔE_p further suggests enhanced apparent electron transfer kinetics at CNT-based electrodes.[22,29,40,55,56] In particular, the Sombers group showed that a different type of CNT yarn microelectrode had an ~2 orders of magnitude increase in the kinetic rate constant, compared to CFMEs.[40] The enhanced electron transfer and the modified adsorption properties at the CNTYME surface present a mass transport profile that is distinct from the profile at the CFME surface. Given the high density of uneven CNTs at the polished electrode surface, cyclic voltammograms of dopamine at the nanostructured surface are likely influenced by a mass transport mechanisms such as thin-film diffusion, as well as adsorption to the CNTYME surface, giving rise to a current dependence on scan frequency that is distinct from CFMEs.[57−59]

Increased Temporal Resolution at High Scan Rates. The typical FSCV scan at a microelectrode has a scan rate of 400 V/s and takes 8.5 ms, so the maximum repetition frequency is ~115 Hz. Increasing the scan rate to 2000 V/s reduces the scan time to 1.7 ms and allows for repetition rates of 500 Hz, which is over 2 orders of magnitude faster than typical FSCV. The CV analysis in Figure 5A shows the large oxidation and reduction peaks measured using the 2000 V/s scan rate and 500 Hz frequency, indicating that FSCV measurements at intervals of 2 ms are possible at CNTYMEs. The current-versus-time curve for dopamine in Figure 5B is similar to curves at the traditional scan and frequency rates (as in Figure 4). The higher scan rate measurements had a temporal response of 0.74 ± 0.07 s when measured at 10 Hz, but the temporal response was 0.29 ± 0.1 s at the 500 Hz sampling frequency. The noise in the current versus time plot increases with higher scan rates; however, the increase in signal is proportional and so the S/N ratio remains at ~110, similar to measurements using 400 V/s and 10 Hz waveform. Thus, CNTYMEs allow the sampling frequency of FSCV measurements to be increased by nearly 2 orders of magnitude and the temporal response is improved by a factor of 4.

Figure 5C shows the oxidation current, measured at 2000 V/s, at frequencies up to 500 Hz ($n = 4$). The horizontal trend of these data indicates that the measured signal is independent of scan frequency, even at fast scan rates. Thus, dopamine can be

dx.doi.org/10.1021/ac404050t | Anal. Chem. 2014, 86, 5721−5727

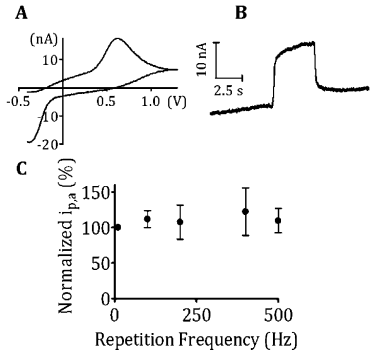

Figure 5. High-frequency measurements of 1 μM dopamine at CNTYMEs: (A) an example background-subtracted CV, and (B) a current-versus-time trace of a 1 μM dopamine injection, measured at 2000 V/s and 500 Hz. (C) The effect of high scan repetition frequencies on the peak oxidation current of 1 μM dopamine at CNTYMEs using a scan rate of 2000 V/s. Data are normalized to the 10 Hz value (n = 4).

measured at intervals of 2 ms without any loss of current, which is a significant advantage for CNTYMEs. However, the higher scan rate also leads to a shift in the measured oxidation and reduction potentials (Figure 5A), which is most likely due to the exaggeration of *iR* drop in the electrochemical cell and bandwidth limitations of the instrument. To limit distortions in potential, proper low-pass filtering must be used, and numerous methods that compensate for *iR* drop and increase instrumental bandwidth could be incorporated to further optimize the high scan rate and high sampling frequency data for ultrafast *in vivo* dopamine measurements.[3,60,61] However, the 2 ms interval is nearly 2 orders of magnitude better than typical FSCV measurements of dopamine at CFMEs, and no instrument modification was required. The sampling interval of FSCV at CNTYMEs is similar to that commonly used with constant potential amperometry, which is often ~1 ms.[62] Therefore, FSCV measurements, which provide chemical information, can now be performed on a time scale similar to that of amperometry.

With FSCV at CFMEs, there is always a tradeoff between sensitivity and time resolution. With CNTYMEs, there is no compromise: high sensitivity, high sampling frequency, and high temporal resolution can be achieved simultaneously. Thus, using CNTYMEs would facilitate experiments that are currently difficult to achieve, such as defining the time course and amount of dopamine release from a single stimulation pulse. High temporal resolution and the high sensitivity measurements at CNTYMEs could also be used to monitor other electroactive neurotransmitters or examine the electrochemical kinetics of other electroactive molecules.

CONCLUSIONS

In summary, we have developed a carbon nanotube yarn microelectrode (CNTYME) capable of measuring changes in dopamine at the 2-ms time scale with fast-scan cyclic voltammetry (FSCV), which is nearly 2 orders of magnitude faster than traditional FSCV measurement rates at carbon-fiber microelectrodes (CFMEs). FSCV at CNTYMEs is comparable to the time scale of measurements using constant potential amperometry. Carbon nanotube (CNT) yarns are an ideal microelectrode material because they are commercially available, have high sensitivity, and have a dopamine oxidation current that is independent of the repetition rate with FSCV. CNTYMEs will be useful for high temporal resolution measurements of neurotransmitters and for monitoring reaction intermediates and kinetic studies of other compounds using FSCV.

ASSOCIATED CONTENT

Supporting Information

Additional details of the experimental methods of surface characterization of the CNTYMEs and additional figures are available in a separate document. The additional figures include maps of the D-band and the G-band Raman peaks across the CNTYME surface (Figure S-1), a TEM image of the MWCNTs that comprise the CNTY (Figure S-2), comparison of the linearity of $i_{p,a}$ with scan rate and the square root of scan rate for $Ir(Cl)_6^{3-}$ (Figure S-3), and determination of the linear range and limit of detection for dopamine at the CNTYME (Figure S-4). This material is available free of charge via the Internet at http://pubs.acs.org.

AUTHOR INFORMATION

Corresponding Author

*Tel.: 434-243-2132. E-mail: bjv2n@virginia.edu.

Author Contributions

The manuscript was written through contributions of all authors. All authors have given approval to the final version of the manuscript.

Notes

The authors declare no competing financial interest.

ACKNOWLEDGMENTS

A portion of this research was conducted at the Center for Nanophase Materials Sciences, (through user grant Nos. CNMS2012-070 and CNMS2014-083), which is sponsored at Oak Ridge National Laboratory by the Scientific User Facilities Division, Office of Basic Energy Sciences, U.S. Department of Energy. This research was funded by the National Science Foundation (NSF) (CHE0645587522) and NIH (Nos. R21DA037584 and R01MH085159).

REFERENCES

(1) Kile, B. M.; Walsh, P. L.; McElligott, Z. A.; Bucher, E. S.; Guillot, T. S.; Salahpour, A.; Caron, M. G.; Wightman, R. M. *ACS Chem. Neurosci.* **2012**, *3*, 285−292.
(2) Viry, L.; Derré, A.; Garrigue, P.; Sojic, N.; Poulin, P.; Kuhn, A. *Anal. Bioanal. Chem.* **2007**, *389*, 499−505.
(3) Hsueh, C. C.; Brajter-Toth, A. *Anal. Chem.* **1993**, *65*, 1570−1575.
(4) Venton, B. J.; Troyer, K. P.; Wightman, R. M. *Anal. Chem.* **2002**, *74*, 539−546.
(5) Huffman, M. L.; Venton, B. J. *Electroanalysis* **2008**, *20*, 2422−2428.
(6) Baur, J. E.; Kristensen, E. W.; May, L. J.; Wiedemann, D. J.; Wightman, R. M. *Anal. Chem.* **1988**, *60*, 1268−1272.
(7) Tang, L.; Zhu, Y.; Xu, L.; Yang, X.; Li, C. *Talanta* **2007**, *73*, 438−443.
(8) Ewing, A. G.; Chen, T. K.; Chen, G. In *Voltammetric and Amperometric Probes for Single Cell Analysis*; Neuromethods, Vol. *27*; Humana Press: Totowa, NJ, 1995; p 63
(9) Goran, J. M.; Lyon, J. L.; Stevenson, K. J. *Anal. Chem.* **2011**, 8123−8129.
(10) Michael, A. C.; Borland, L.; Borland, L. M. *Electrochemical Methods for Neuroscience*; CRC Press: Boca Raton, FL, 2007; p 512.
(11) Robinson, D. L.; Venton, B. J.; Heien, M. L. A. V; Wightman, R. M. *Clin. Chem.* **2003**, *49*, 1763−1773.

(12) Heien, M. L. A. V; Johnson, M. A.; Wightman, R. M. *Anal. Chem.* **2004**, *76*, 5697−5704.
(13) Robinson, D. L.; Hermans, A.; Seipel, A. T.; Wightman, R. M. *Chem. Rev.* **2008**, *108*, 2554−2584.
(14) Kawagoe, K. T.; Zimmerman, J. B.; Wightman, R. M. *J. Neurosci. Methods* **1993**, *48*, 225−240.
(15) Nguyen, M. D.; Lee, S. T.; Ross, A. E.; Ryals, M.; Choudhry, V. I.; Venton, B. J. *PLoS One* **2014**, *9*, e87165.
(16) Hu, C.; Hu, S. *Langmuir* **2008**, *24*, 8890−8897.
(17) McCreery, R. L. *Chem. Rev.* **2008**, *108*, 2646−2687.
(18) Chen, P.; Fryling, M. A.; Mccreery, R. L. *Anal. Chem.* **1995**, *67*, 3115−3122.
(19) Jacobs, C. B.; Peairs, M. J.; Venton, B. J. *Anal. Chim. Acta* **2010**, *662*, 105−127.
(20) Banks, C. E.; Davies, T. J.; Wildgoose, G. G.; Compton, R. G. *Chem. Commun. (Cambridge, U.K.)* **2005**, 829−841.
(21) Gong, K.; Chakrabarti, S.; Dai, L. *Angew. Chem., Int. Ed. Engl.* **2008**, *47*, 5446−5450.
(22) Swamy, B. E. K.; Venton, B. J. *Analyst* **2007**, *132*, 876−884.
(23) Jacobs, C. B.; Vickrey, T. L.; Venton, B. J. *Analyst* **2011**, *136*, 3557−3565.
(24) Wang, J.; Deo, R. P.; Poulin, P.; Mangey, M. *J. Am. Chem. Soc.* **2003**, *125*, 14706−14707.
(25) Atthipalli, G.; Epur, R.; Kumta, P. N.; Yang, M.; Lee, J.-K.; Gray, J. L. *J. Phys. Chem. C* **2011**, *115*, 3534−3538.
(26) Liu, X.; Baronian, K. H. R.; Downard, A. J. *Anal. Chem.* **2008**, *80*, 8835−8839.
(27) Wang, J. *Electroanalysis* **2005**, *17*, 7−14.
(28) Banks, C. E.; Compton, R. G. *Analyst* **2006**, *131*, 15.
(29) Dumitrescu, I.; Unwin, P. R.; Macpherson, J. V. *Chem. Commun. (Cambridge, U.K.)* **2009**, *7345*, 6886−6901.
(30) Xiao, N.; Venton, B. J. *Anal. Chem.* **2012**, *84*, 7816−7822.
(31) Li, W.; Jayasinghe, C.; Shanov, V.; Schulz, M. *Materials (Basel)* **2011**, *4*, 1519−1527.
(32) Jakubinek, M. B.; Johnson, M. B.; White, M. A.; Jayasinghe, C.; Li, G.; Cho, W.; Schulz, M. J.; Shanov, V. *Carbon* **2012**, *50*, 244−248.
(33) Jayasinghe, C.; Amstutz, T.; Schulz, M. J.; Shanov, V. *J. Nanomater.* **2013**, *2013*, 1−7.
(34) Sears, K.; Skourtis, C.; Atkinson, K.; Finn, N.; Humphries, W. *Carbon* **2010**, *48*, 4450−4456.
(35) Jiang, C.; Li, L.; Hao, H. *IEEE Trans. Neural Syst. Rehabil. Eng.* **2011**, *19*, 612−616.
(36) Zhu, Z.; Garcia-Gancedo, L.; Flewitt, A. J.; Moussy, F.; Li, Y.; Milne, W. I. *J. Chem. Technol. Biotechnol.* **2012**, *87*, 256−262.
(37) Zhu, Z.; Song, W.; Burugapalli, K.; Moussy, F.; Li, Y.-L.; Zhong, X.-H. *Nanotechnology* **2010**, *21*, 165501.
(38) Wu, H.-C.; Chang, X.; Liu, L.; Zhao, F.; Zhao, Y. *J. Mater. Chem.* **2010**, *20*, 1036.
(39) Zhao, H.; Zhang, Y.; Bradford, P. D.; Zhou, Q.; Jia, Q.; Yuan, F.-G.; Zhu, Y. *Nanotechnology* **2010**, *21*, 305502.
(40) Schmidt, A. C.; Wang, X.; Zhu, Y.; Sombers, L. A. *ACS Nano* **2013**, 7864−7873.
(41) Clark, J. J.; Sandberg, S. G.; Wanat, M. J.; Gan, J. O.; Horne, E. A.; Hart, A. S.; Akers, C. A.; Parker, J. G.; Willuhn, I.; Martinez, V.; Evans, S. B.; Stella, N.; Phillips, P. E. M. *Nat. Methods* **2010**, *7*, 126−129.
(42) Strand, A. M.; Venton, B. J. *Anal. Chem.* **2008**, *80*, 3708−3715.
(43) Hendricks, T. R.; Ivanov, I. N.; Schaeffer, D. A.; Menchhofer, P. A.; Simpson, J. T. *Nanotechnology* **2010**, *21*, 115301.
(44) Antunes, E. F.; Lobo, A. O.; Corat, E. J.; Trava-Airoldi, V. J. *Carbon* **2007**, *45*, 913−921.
(45) Antunes, E. F.; Lobo, A. O.; Corat, E. J.; Trava-Airoldi, V. J.; Martin, A. A.; Veríssimo, C. *Carbon* **2006**, *44*, 2202−2211.
(46) Wang, Y.; Alsmeyer, D. C.; McCreery, R. L. *Chem. Mater.* **1990**, *2*, 557−563.
(47) Bowling, R. J.; Packard, R. T.; McCreery, R. L. *J. Am. Chem. Soc.* **1989**, *111*, 1217−1223.
(48) Bokobza, L. *Express Polym. Lett.* **2012**, *6*, 601−608.
(49) Nakamizo, M.; Tamai, K. *Carbon* **1984**, *22*, 197−198.
(50) Ivanov, I.; Puretzky, A.; Eres, G.; Wang, H.; Pan, Z.; Cui, H.; Jin, R.; Howe, J.; Geohegan, D. B. *Appl. Phys. Lett.* **2006**, *89*, 223110.
(51) Ferrari, a.; Robertson, J. *Phys. Rev. B* **2000**, *61*, 14095−14107.
(52) Bard, A. J.; Faulkner, L. R. *Electrochemical Methods: Fundamentals and Applications*, 2nd Edition.; John Wiley & Sons: New York, 2001.
(53) McCreery, R. L.; Cline, K. K.; McDermott, C. A.; McDermott, M. T. *Colloids Surf., A* **1994**, *93*, 211−219.
(54) Bath, B. D.; Michael, D. J.; Trafton, B. J.; Joseph, J. D.; Runnels, P. L.; Wightman, R. M. *Anal. Chem.* **2000**, *72*, 5994−6002.
(55) Hocevar, S. B.; Wang, J.; Deo, R. P.; Musameh, M.; Ogorevc, B. *Electroanalysis* **2005**, *17*, 417−422.
(56) Jacobs, C. B.; Vickrey, T. L.; Venton, B. J. *Wiley Encycl. Chem. Biol.* **2008**, 1−12.
(57) Streeter, I.; Wildgoose, G. G.; Shao, L.; Compton, R. G. *Sens. Actuators, B* **2008**, *133*, 462−466.
(58) Henstridge, M. C.; Dickinson, E. J. F.; Aslanoglu, M.; Batchelor-McAuley, C.; Compton, R. G. *Sens. Actuators, B* **2010**, *145*, 417−427.
(59) Henstridge, M. C.; Compton, R. G. *Chem. Rec.* **2012**, *12*, 63−71.
(60) Keithley, R. B.; Takmakov, P.; Bucher, E. S.; Belle, A. M.; Owesson-White, C. A.; Park, J.; Wightman, R. M. *Anal. Chem.* **2011**, *83*, 3563−3571.
(61) Hermans, A.; Keithley, R. B.; Kita, J. M.; Sombers, L. A.; Wightman, R. M. *Anal. Chem.* **2008**, *80*, 4040−4048.
(62) Dugast, C.; Suaud-Chagny, M. F.; Gonon, F. *Neuroscience* **1994**, *62*, 647−654.